Land surface predictability in Europe: Extremes and trends

Eric B. Jaeger and Sonia I. Seneviratne

ETH, Institute for Atmospheric and Climate Science, Zurich
8092, Switzerland
eric.jaeger@env.ethz.ch, sonia.seneviratne@env.ethz.ch

ABSTRACT

For mid-range and seasonal weather forecasting as well as for climate projections, the importance of soil moisture as lower boundary condition for the atmosphere is being increasingly recognized. This is mostly due to the role of soil moisture as storage component for heat and moisture. The associated memory induces persistence in the overlying atmosphere. This has potential consequences for long-term forecasting, but only in regions where the atmosphere is coupled to the underlying land surface. This extended abstract provides an overview on diagnostics of land-atmosphere coupling and on a recent study (Jaeger and Seneviratne, 2009) assessing the sensitivity of the European summer climate to soil moisture using a regional climate model.

1 Introduction

Soil moisture (SM) is a key variable of the climate system because of its impacts on the surface energy and water balances. This has consequences for the near-surface climate (temperature, humidity) as well as for boundary-layer processes (e.g. convective precipitation) and potentially also large-scale circulation patterns. Moreover, as a storage component for water and hence indirectly also for energy, it represents an important memory component for the regional climate system, with high potential for seasonal forecasting. It is however not routinely measured in most parts of the world, particularly in Europe, where measurement datasets are scarce [*Seneviratne et al.*, 2009].

Since climate extremes have a major societal, economical, and ecological impact, they are of particular interest for society. Several observational [*Della-Marta et al.*, 2007] and modeling studies [*Meehl and Tebaldi*, 2004] report an increase in temperature extremes in mid-latitude regions with climate change, that can be linked (among other factors) to changes in soil moisture regimes [*Seneviratne et al.*, 2006]. However, soil moisture only impacts the surface climate in specific regions on earth, so called 'hot-spots' of land-atmosphere coupling [*Koster et al.*, 2004]. Since large-scale field experiments investigating land-atmosphere coupling effects are not feasible, one way of assessing the underlying mechanisms is to run climate model experiments.

Hereafter, we discuss results from a study assessing the sensitivity of temperature extremes and trends to the soil moisture state. Our study uses output from regional climate model simulations run for the last 50 years over the European continent. The applied methodology is based on simulations with prescribed and interactive SM (similar as in e.g. *Koster et al.* [2004] and *Seneviratne et al.* [2006]). This approach allows us to assess the impact of SM on climate by decoupling the land-surface part of the model from the atmospheric part, and thereby to infer causal relationships. In the simulations with prescribed SM the two-way coupling of the atmosphere and SM is removed, and the experiments thus investigate only the one-way effect of SM on the atmosphere, whereas the atmosphere has no influence on SM.

The outline of this extended abstract is as follows: Section 2 reviews studies investigating the location of regions of strong land atmosphere-coupling. Then, in Section 3, the sensitivity of temperature extremes and trends to soil moisture is assessed in a modeling framework. Implications of these results for weather and seasonal forecasting and related on-going projects in Switzerland are discussed in Section 4.

2 Hot spots of land-atmosphere coupling

Accurate seasonal forecasts are based on the atmospheric response to slowly varying states of the ocean and the land surface, which can be predicted months in advance. The landmark GLACE-1 study of *Koster et al.* [2004] has derived a global map of so called 'hot-spots' of land-atmosphere coupling from numerical experiments with state-of-the-art General Circulation Models (GCMs). The location of these regions indicate where the routine monitoring of soil moisture could possibly be used for model initialization to improve the skill for seasonal climate predictions. The identified hot-spots are found to be mainly located in transitional zones between dry and wet climate, where evapotranspiration is sensitive to soil moisture and its variations are large enough to impact climate significantly.

Figure 1 displays the GLACE-1 Ω-diagnostic for temperature and precipitation (top row), together with other land-atmosphere coupling diagnostics. The second row displays the correlation of temperature (T) and evapotranspiration (E) ($\rho_{T,E}$) proposed by *Seneviratne et al.* [2006], and applied to IPCC AR4 simulations for the time periods 1970-1989 (middle left) and 2080-2099 (middle right). Negative values of $\rho_{T,E}$ are indicative of strong soil moisture-temperature coupling, whereas positive $\rho_{T,E}$ are generally associated with an atmospheric control on E. Finally, the bottom row provides estimates of the drivers of evapotranspiration using the correlations $\rho_{P,E}$ and/or $\rho_{R_g,E}$, which allows to distinguish between water- (P denotes precipitation in $\rho_{P,E}$) and energy-limited (R_g denotes global radiation in $\rho_{R_g,E}$) evapotranspiration regimes [*Teuling et al.*, 2009]. Water-limited evapotranspiration regimes are associated with positive values of $\rho_{P,E}$ (only applicable on annual scale), whereas radiation-limited regimes are generally associated by positive $\rho_{R_g,E}$. The bottom left figure displays a combined analysis of the $\rho_{P,E}$ and $\rho_{R_g,E}$ diagnostics applied on annual scale to simulations from the Global Soil Wetness Project (GSWP, *Dirmeyer et al.* [2006]), while the bottom right figure displays (daily) $\rho_{R_g,E}$ for the months May-September applied to measurements from the FLUXNET network [*Baldocchi et al.*, 2001].

Despite being based on several different approaches and datasets, the diagnostics for present-day climate in Fig. 1 (top row, middle left, bottom row) all display a consistent picture. The Great Plains of North America are found as being moisture rather than radiation limited (bottom analyses), and accordingly, also show a strong land-atmosphere coupling strength both on intra-annual (top, GLACE-1) and interannual time scales (middle left, IPCC AR4). Over Europe, the IPCC, GSWP and Fluxnet analyses suggest the presence of another hot spot of land-atmosphere coupling in the Mediterranean region. This hot spot was not identified in the GLACE-1 study, which may have been due to its set-up based on a single climatic year [*Seneviratne et al.*, 2006]. However, all diagnostics suggest that Central and Northern Europe has a radiation-limited climate regime, and thus low land-atmosphere coupling for present climate. This is diagnosed to be changed under future-climatic conditions (middle right), due to a shift in soil moisture regime in this region. One should further note that several studies have suggested that even for recent decades in Central Europe, and in particular France, soil moisture can play an important part in extreme years regarding the occurrence of summer heat waves [e.g. *Fischer et al.* 2007, *Vautard et al.* 2007], highlighting that the boundary between moisture- and radiation-limited climate zones is labile and also dependent on the considered time scale. In the following section, we further investigate the role of SM for temperature extremes and trends in Europe using sensitivity experiments performed with a regional climate model.

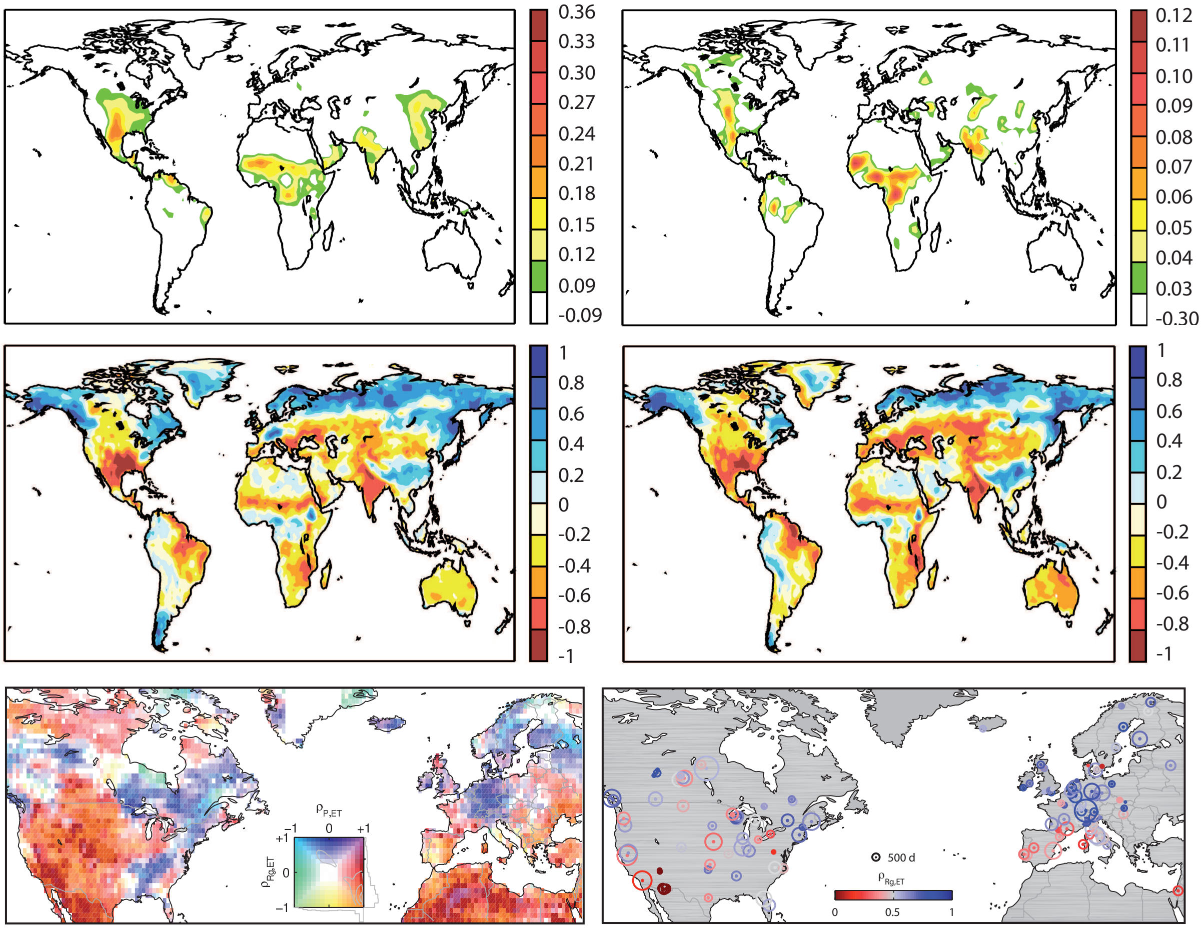

Figure 1: Top row: Estimations of the soil moisture-temperature (left panel) and soil moisture-precipitation (right panel) coupling, based on the Ω-coupling diagnostic and on the output of 12 GCMs from the GLACE-1 project (after Koster et al. [2006]). Middle row: Estimations of soil moisture-temperature coupling for 1970-1989 (left panel) and 2080-2099 (right panel) climates, based on 3 IPCC GCMs and diagnosed with $\rho_{T,E}$ (after Seneviratne et al. [2006]). Bottom row: Estimation of the drivers of E (moisture and radiation; after Teuling et al. [2009]). The left panel is based on simulations from the GSWP project [Dirmeyer et al., 2006] and shows controls on yearly E, whereas the right panel displays the observed radiative control on daily E based on Fluxnet data [Baldocchi et al., 2001].

3 Impact of soil moisture on the European summer climate

Hereafter, we briefly summarize some of the highlights of a recently submitted paper [*Jaeger and Seneviratne*, 2009] that deals with the impact of different soil moisture settings on the European summer climate using the regional climate model CLM. Thereby, the focus is particularly set on the impact of SM on climate extremes and trends.

3.1 Introduction and modeling setup

The study uses the CLM RCM, which is the climate version of the non-hydrostatic COSMO model (COnsortium for Small-scale MOdeling: http://cosmo-model.cscs.ch/). A similar model configuration is adopted as for the EU-FP6 project ENSEMBLES (http://www.ensembles-eu.org) validated in *Jaeger et al.* [2008]. In addition, the employed model setup was validated with regard to land-atmosphere coupling characteristics with FLUXNET observations in *Jaeger et al.* [2009]. CLM is integrated over the European continent, with 0.44° (≈ 50 km) horizontal resolution, 32 levels in the vertical and 10 soil layers. Lateral boundary conditions are derived from the ERA40 re-analysis (1958-2001, *Uppala et al.* [2005]) and from ECMWF operational analysis (2002-2006). The applied CLM configuration uses the Tiedtke convection scheme based on a moisture-convergence closure, which was shown to have a strong sensitivity of precipitation to evapotranspiration anomalies [*Brockhaus et al.*, 2009; *Jaeger and Seneviratne*, 2009]. Details on the model dynamics and physics are provided in the model documentation (available from: http://www.clm-community.eu/).

In order to assess the possible impact of extreme values and of the temporal variability of SM on the European summer climate, a set of sensitivity experiments with different prescribed SM evolutions was performed (see Fig. 2 for an illustration of the SM values of the sensitivity experiments in comparison with the control simulation). Note that in the prescribed SM experiments, soil moisture is not altered by any surface fluxes, nor by precipitation or runoff. A reference simulation includes interactive SM, and will be referred to as CTL hereafter. Two sensitivity experiments were performed with minimum (plant wilting point, PWP) and maximum (field capacity, FCAP) soil moisture values. In addition, the impact on climate of temporal SM variability on different time scales is assessed. In order to disentangle the effects of synoptic-scale, intraseasonal, and interannual SM variability, the soil moisture time series from CTL are subsequently filtered using a digital low-pass filter. A first experiment removes the synoptic-scale variability (called SSV) of SM; A second experiment additionally removes the intraseasonal variability (called ISV) from SSV; A third experiment also removes the interannual variability from ISV (called IAV).

3.2 Impact on extremes

While in *Jaeger and Seneviratne* [2009] several diagnostics for extreme events are assessed, we will focus hereafter only on heat wave duration indices (Fig. 3) as well as on the analysis of the PDFs of daily maximum temperatures (T_{max}, Fig. 4).

Figure 3 (top left panel) displays the mean heat wave duration index $hwdi_{mean}$ that assesses the atmospheric tendency for persistence at the upper tail of the daily T_{max} distribution. It is calculated as the mean of all events with at least two consecutive days of T_{max} above the long-term 90^{th}-percentile of the CTL simulation. The 90^{th}-percentile of each summer day is calculated from samples of 5days (2 days before and 2 days after) over the full analysis period (1959-2006). Largest values occur in the Mediterranean and in Eastern and Northern Europe. Generally, the values of $hwdi_{mean}$ are higher for regions neighbouring oceans, possibly indicating an effect of persistence associated with SSTs. A comparison of the differences of $hwdi_{mean}$ between the sensitivity and CTL experiments yields the following: There

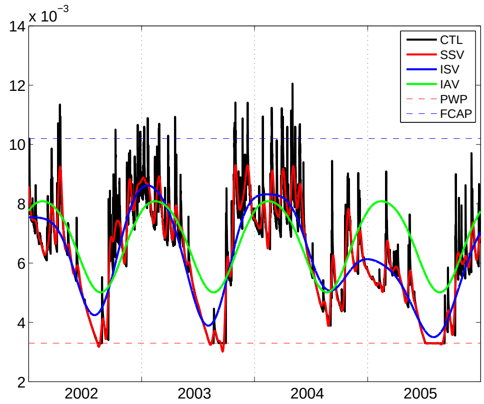

Figure 2: Illustration of the soil moisture evolution of the different CLM experiments for a grid point from the Iberian Peninsula. Shown is the 2^{nd} model soil level for the period 2002-2005.

is a continuous decrease from SSV over ISV to IAV, and most pronounced effects in FCAP and PWP (Fig. 3, top panels). It is likely that one cannot trust the strong impact of SM on the heat wave indices in Scandinavia, since *Jaeger et al.* [2009] found a poor representation of land-atmosphere coupling in Northern Europe in the applied CLM version. Finally, note that the biases of temperature extremes of CTL are comparable to those of current state-of-the-art RCMs from ENSEMBLES (see also *Jaeger and Seneviratne* [2009]).

The index $hwdi^{\star}_{mean}$ (Fig. 3, bottom panels) is an indirect measure of intrinsic heat wave persistence. In contrast to $hwdi_{mean}$, it uses the long-term 90^{th}-percentile of the respective simulation as threshold for the definition of heat wave days. If one compares $hwdi^{\star}_{mean}$ in two simulations, differences in this index can (mostly) only arise from the fact that the clustering of days above their respective 90^{th}-percentile differs (in both simulations 10% of all days are above the 90^{th}-percentile). As shown in Fig. 3 $hwdi^{\star}_{mean}$ exhibits clear reductions in the IAV, PWP and FCAP experiments. A more thorough analysis reveals that this is in line with a decrease in the autocorrelation of T_{max}, and that the distribution of the length of 90^{th}-percentile threshold exceedances shows an increase of shorter and a decrease of longer lasting heat wave episodes (for further details see *Lorenz et al.* [2009]). This can be understood by the fact that in these simulations precipitation does not cause SM anomalies (prescribed SM). Hence, one source of atmospheric persistence, namely soil moisture memory, is shut down. We see from the response of the IAV experiment that it is the memory associated with interannual SM anomalies that is mostly relevant.

In Fig. 4 (left panel) we assess the PDFs of mean subdomain daily T_{max} in France, using the subdomain definition of the EU-project PRUDENCE [e.g. *Christensen and Christensen, 2007*]. Analyses for other European subdomains are provided in the supplementary information of *Jaeger and Seneviratne* [2009]. Consistent with the previous analysis of the $hwdi_{mean}$ and $hwdi^{\star}_{mean}$ heat wave indices, largest differences of daily T_{max} are found for PWP and FCAP. The analysis reveals that the T_{max} PDFs of the PWP and FCAP simulations are significantly different from CTL (based on the two-sided Kolmogorov-Smirnov test, with $\alpha = 5\%$), which to a lesser extent also holds for ISV and IAV. At least for PWP, FCAP and IAV, not only the mean but also the tails or the spread of the distributions are significantly smaller. Interestingly, PWP (FCAP) exhibits a pronounced widening (narrowing) of its PDF, which is due to the removed (increased) damping effect of SM – through latent cooling – on the temperature extremes at the high end (i.e. hot extremes). The distinct impact of SM is clearly recognizable from the asymmetric effects on the PDFs.

The right panel of Fig. 4 displays the corresponding PDFs of the extreme value distribution of daily T_{max} (using the Generalized Extreme Value distribution (GEV) based on the block maxima approach [*Coles*,

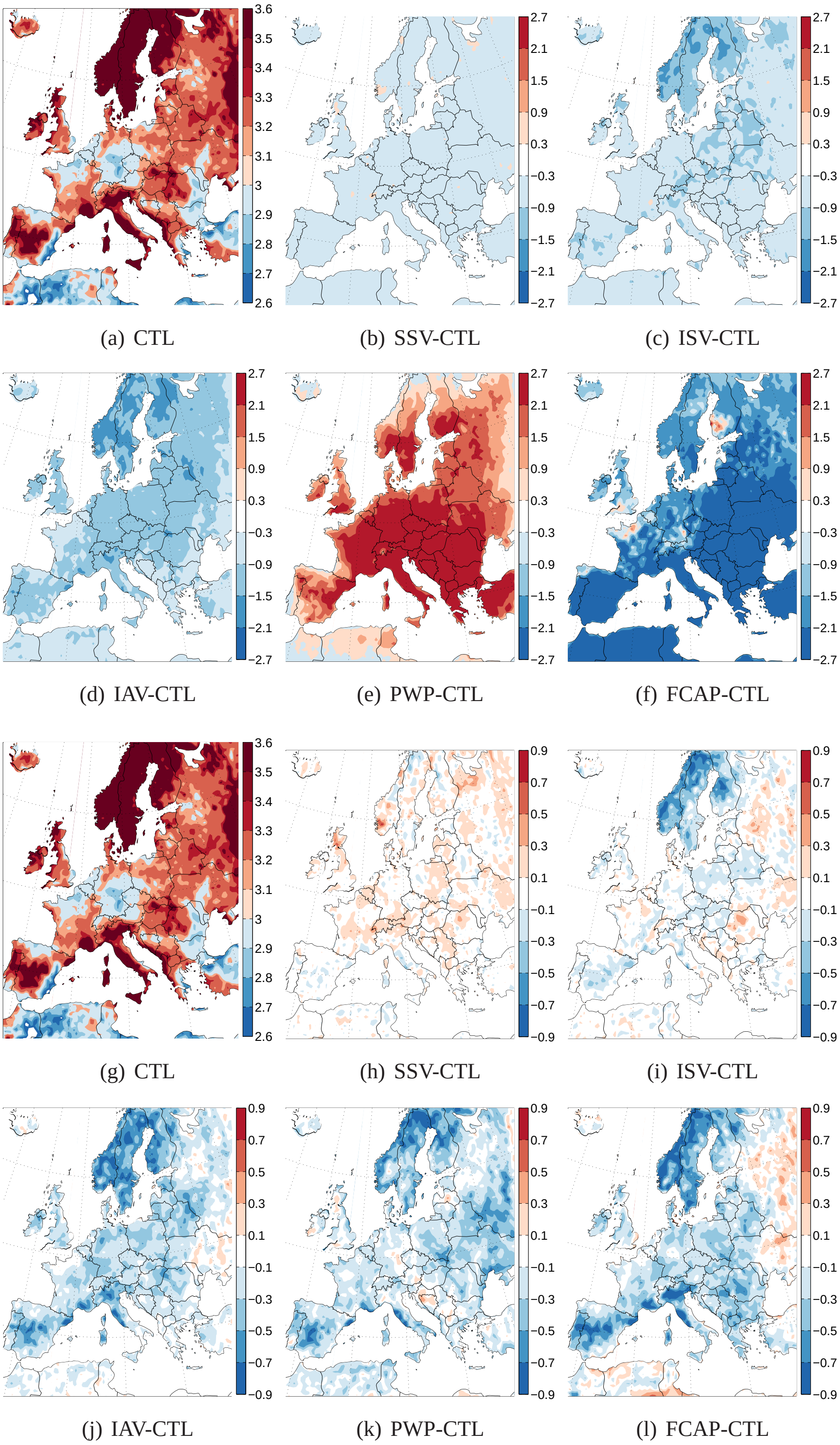

Figure 3: Summer climatologies (1959-2006) of the impact of SM variability on T_{max} extreme diagnostics: $hwdi_{mean}$ (heat wave day threshold defined with respect to 90^{th}-percentile of CTL, [d], 1^{st} and 2^{nd} row) and $hwdi^{\star}_{mean}$ (heat wave day threshold defined with respect to 90^{th}-percentile of respective experiment, [d], 3^{rd} and 4^{th} row).

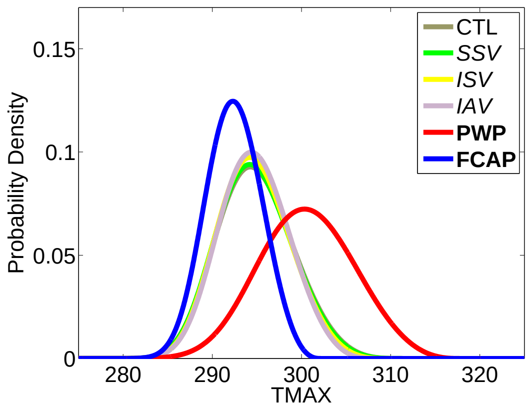

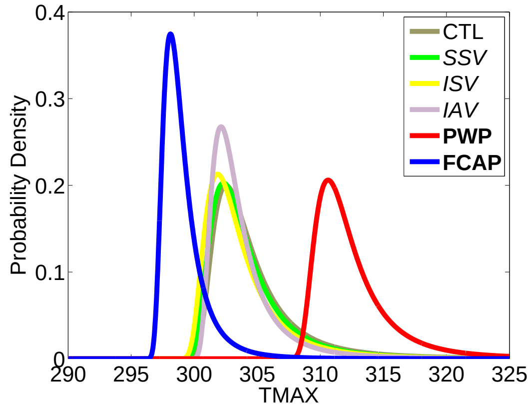

Figure 4: PDFs of daily T_{max} [K] (left) and of summer T_{max} block maximas [K] (right) using a GEV fit in both cases. The PDFs are based on the mean French subdomain values and the summer period 1959-2006. Simulations with bold legend entries are significantly different from CTL at the 5% level according to the two-sided Kolmogorov-Smirnov test.

2001]). These PDFs are shifted to higher temperatures and they are narrower compared to the PDFs of daily T_{max} discussed above. While the differences of the sensitivity experiments seem to be more pronounced, the statistical analysis reveals slightly lower significance (mainly due to the smaller sample size). As identified for the overall PDFs, we see that SM has a strong impact mainly on temperature maxima (the higher tails of the PDFs), which can be understood from the presence or lack of latent cooling.

In summary, we find that reducing the temporal soil moisture variability reduces the temperature extremes, and that it is the interannual variability of SM that is most relevant in this respect. Imposing extreme values of soil moisture has the largest impact. These effects are asymmetric and impact temperature maxima rather than the whole PDF, which is consistent with a non-linear dependency of surface fluxes on soil moisture [e.g. *Koster et al.*, 2004, *Seneviratne et al.*, 2009], i.e. the existence of distinct regimes with little vs. high sensitivity to soil moisture (in wet, respectively drier, soil moisture conditions).

3.3 Impact on trends

In this section we investigate trends in summer climate over the period 1959-2006 in the conducted experiments. Of particular interest is the question of whether changes in soil moisture characteristics may have any influence on these trends. Using the performed CLM experiments with and without prescribed SM, this can be easily assessed. We discuss here only the results for T_{max} and cloud cover. Further results are provided in *Jaeger and Seneviratne* [2009].

The analysis reveals that the trends are different for simulations with (CTL, SSV, ISV) and without (IAV, PWP, FCAP) SM trends, respectively. However, since there are no substantial differences (not shown) between trends for CTL, SSV and ISV, respectively IAV, PWP and FCAP, we only discuss here the trends for CTL and IAV.

We distinguish here two periods corresponding to the 'global-dimming/global-brightening' phases [e.g. *Wild et al.*, 2004]: 1959-1980 ('1st period') and 1981-2006 ('2nd period'). Figure 5 shows that there is a striking temporal variation in the Theil-Sen's trend estimates (trend estimator from the Mann-Kendall tau trend test) for the mean of daily T_{max} between the 1st and 2nd periods. For CTL there is a negative trend for the 1st period over the whole of Europe, and a positive trend for the 2nd period. For IAV there is a tendency for smaller negative and positive trends for the 1st and 2nd period, respectively (the numbers in the lower right corner denote the area-weighted fraction of land points with statistically significant trends according to the Mann-Kendall tau test, at the 10% level).

The corresponding trends for T_{min} exhibit similar spatial and temporal patterns but are weaker. Moreover, the differences between CTL and IAV are substantially smaller. Hence, SM (trends) unequally affect T_{max} and T_{min} (trends), with consequences for the DTR trends (not shown, see *Jaeger and Seneviratne* [2009]).

Interestingly, these contrasting trends over the two analysed periods are found despite the fact that CLM does not explicitly include changes in aerosol concentrations. These are also not included in the driving boundary conditions (ERA40, ECMWF operational analysis). However, part of the local response could be due to changes in cloud cover due to the imposed boundary conditions (i.e. changes in moisture or temperature fields - which could be indirectly due to aerosol trends - captured in the reanalysis/analysis datasets thanks to data assimilation).

Therefore, we also investigate the trends in CLM total cloud cover in Fig. 5. They exhibit the same spatial as well as temporal patterns (with an increase in the 1st period and a decrease thereafter) as the trends in daily T_{max}. The SM trend patterns (both spatial and temporal) are similar to those of the cloud cover (not shown). Since cloud cover and SM interact with one another, it is difficult to assess their respective independent contributions to the temperature trends. However, by looking at those simulations without trends in SM, one finds a small trend reduction (in particular for extreme values of T_{max}, not shown). Therefore, we conclude that in CLM the trends of daily T_{max} and of DTR (not shown) are mainly due to trends in cloud cover caused by the large-scale forcing (circulation patterns, as well as temperature and relative humidity of incoming air at the domain boundaries), and that SM has an amplifying effect. Finally, note that despite inconsistencies in the boundary data (e.g. the change from ERA40 re-analysis to ECMWF operational analysis in 2002, or the inclusion of satellite data assimilation in recent decades), a comparison with observed trends reveals a reasonable representation, at least qualitatively (see *Jaeger and Seneviratne* [2009]).

4 Implications for weather and seasonal forecasting

As discussed in the two previous sections, soil moisture is a key variable of the climate system that is likely to become even more crucial in future climate in regions such as Central Europe [*Seneviratne et al.*, 2006]. Our results suggest that this is particularly the case for extreme (hot) temperature events. Given their relevance for society, this highlights some key perspectives for the development of weather and seasonal forecasting applications relying on soil moisture initialization.

However, one major impediment for using soil moisture information in forecasting system is that only few large-scale and long-term soil moisture networks are available so far [*Seneviratne et al. 2009*]. This is particularly the case in Europe. This lack of ground measurements inhibits the evaluation of weather forecasting and climate models with respect to land surface processes, and of data assimilation schemes for satellite soil moisture retrievals.

Based on these shortcomings ETH Zurich in collaboration with Agroscope and MeteoSwiss are currently conducting an ambitious three-year (2008-2011) soil moisture monitoring experiment (Swiss SMEX: The Swiss Soil Moisture Experiment http://www.iac.ethz.ch/groups/seneviratne/research/SwissSMEX). The project encompasses 15 sites in Switzerland that will allow a comprehensive assessment of soil moisture in this region. Among other, this projects aims at assessing the following issues: The determination of the impact of soil moisture for the local and regional climate (feedbacks) and of its potential for weather and seasonal forecasting in Switzerland, and the validation of land surface and climate

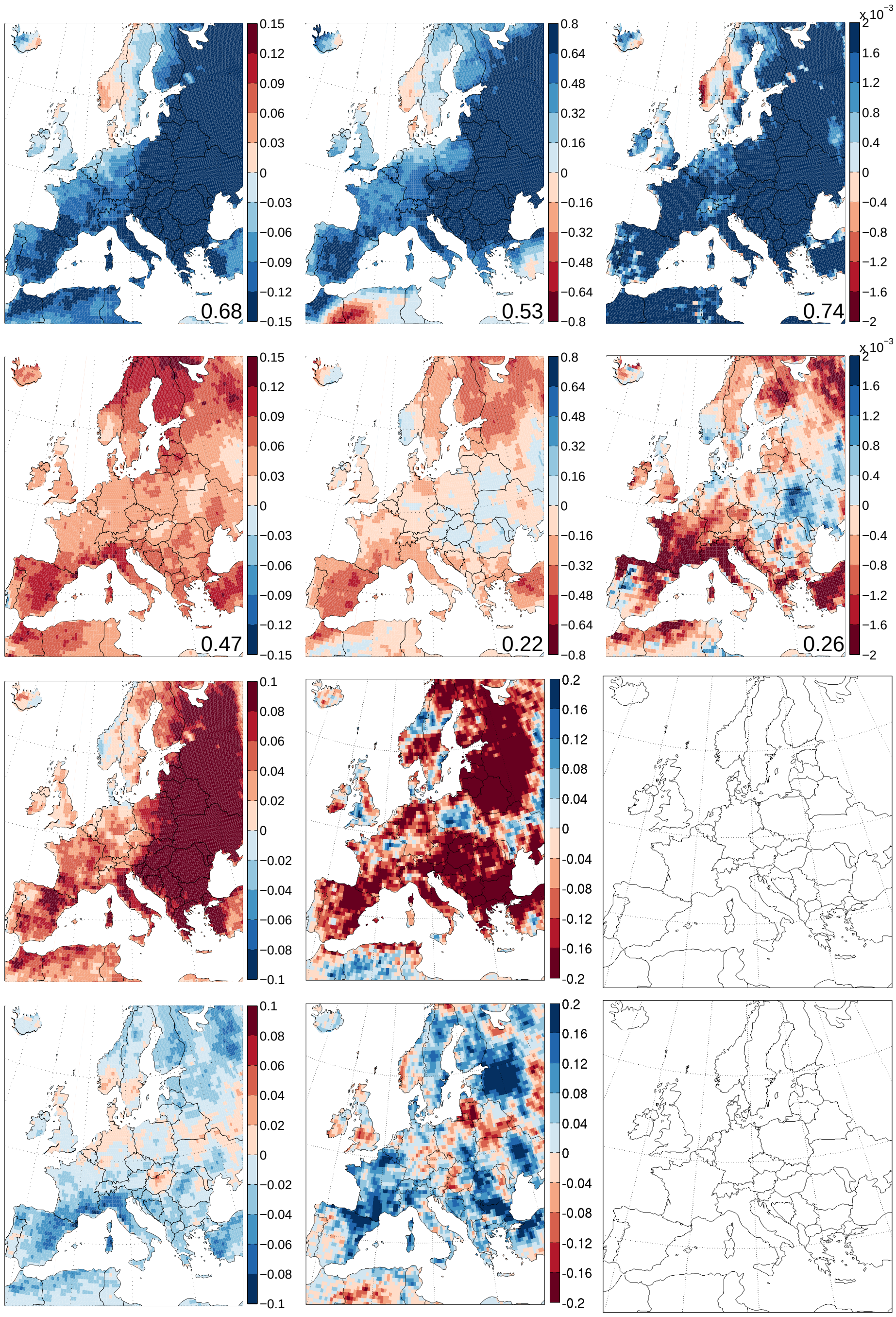

Figure 5: From left to right: Linear trends as expressed by Theil-Sen's trend estimate for mean daily T_{max} [K/y], total cloud cover [%/y], and soil moisture [m/y]. The 1st row displays the 1. summer period 1959-1980, the 2nd row the 2. summer period 1981-2006 for CTL. The 3rd and 4th rows give the same but for IAV-CTL.

models with regard to soil moisture representation in Central Europe. This project will also be complemented by a further project focusing more specifically on the early warning and prediction of droughts in Switzerland, DROUGHT-CH, which will be conducted from 2010-2012 in the framework of the NRP61 program on sustainable water management (http://www.nfp61.ch/E/Pages/home.aspx).

Our results suggest that initiatives investigating more specifically the potential of soil moisture initialization for extreme events should be further developed in several regions, and in particular in Europe, where they have not been thoroughly assessed so far. Applications on longer time scales (e.g. decadal forecasting, climate-change projections) are also important given the key role of SM for climate trends.

Acknowledgements

This research was supported through the EU-FP6 project CECILIA (contract number 037005) and ETH Zurich. The CLM simulations have been conducted at the Swiss National Supercomputing Centre (CSCS). We are indebted to the COSMO and CLM communities, as well as to MeteoSwiss and ECMWF, for providing access to and support for the CLM and the ERA40 reanalysis/ECMWF operational analysis, respectively. The following members of the land-climate interactions research group at ETH Zurich contributed comments and/or figures for this extended abstract: Ryan Teuling, Heidi Mittelbach, Martin Hirschi and Ruth Lorenz.

References

[1] Baldocchi, D., et al. (2001), FLUXNET: A new tool to study the temporal and spatial variability of ecosystem-scale carbon dioxide, water vapor, and energy flux densities, *Bull. Am. Meteorol. Soc.*, *82*, 2415-2433.

[2] Brockhaus, P., P. Bechthold, O. Fuhrer, D. Lüthi, and C. Schär (2009), The ECMWF IFS convection scheme applied to the COSMO limited-area model, *Quart. J. Roy. Meteor. Soc.*, submitted.

[3] Christensen, J. H, and O. B. Christensen (2007), A summary of the PRUDENCE model projections of changes in European climate during this century, *Clim. Change*, doi:10.1007/s10584-006-9210-7.

[4] Coles, S. G. (2001), An introduction to statistical modeling of extreme values. Springer Series in Statistics, Springer, 224pp.

[5] Della-Marta, P. M., M. R. Haylock, J. Luterbacher, and H. Wanner (2007), Doubled length of western European summer heat waves since 1880, *J. Geophys. Res.*, *112*, D15103, doi:10.1029/2007JD008510.

[6] Dirmeyer P. A., X. Gao, M. Zhao, Z. Guo, T. Oki, N. Hanasaki (2006), GSWP-2: Multimodel analysis and implications for our perception of the land surface, *B. Am. Meteorol. Soc. 87*, 13811397.

[7] Fischer, E. M., S. I. Seneviratne, D. Lüthi, and C. Schär (2007), Contribution of land-atmosphere coupling to recent European summer heat waves, *Geophys. Res. Lett.*, *34*, L06707, doi:10.1029/2006GL0 29068.

[8] Jaeger, E. B., I. Anders, D. Lüthi, B. Rockel, C. Schär, and S. I. Seneviratne (2008), Analysis of ERA40-driven CLM simulations for Europe, *Meteorol. Z.*, *17*, 349-367.

[9] Jaeger, E. B., R. Stöckli, and S. I. Seneviratne (2009), Analysis of planetary boundary layer fluxes and land-atmosphere coupling in the Regional Climate Model CLM, *J. Geophys. Res.*, *114*, D17106, doi:10.1029/2008JD011658.

[10] Jaeger, E. B., and S. I. Seneviratne (2009), Impact of soil moisture-atmosphere coupling on European climate extremes and trends in a regional climate model, *Clim. Dynam.*, submitted.

[11] Koster, R. D. et al. (2004), Regions of strong coupling between soil moisture and precipitation, *Science, 305*, 1138-1140.

[12] Koster, R. D. et al. (2006), GLACE: The Global Land-Atmosphere Coupling Experiment. Part I: Overview, *J. Hydrometeor., 7*, 590-610.

[13] Lorenz R., E. B. Jaeger, and S. I. Seneviratne (2009), Persistence of heat waves and its link to soil moisture memory, *Geophys. Res. Lett.*, submitted.

[14] Meehl, G. A., and C. Tebaldi (2004), More Intense, More Frequent, and Longer Lasting Heat Waves in the 21st Century, *Science, 305*, 994 - 997.

[15] Seneviratne, S. I., D. Lüthi, M. Litschi, and C. Schär (2006), Land-atmosphere coupling and climate change in Europe, *Nature, 443*, 205-209.

[16] Seneviratne, S. I., T. Corti, E. L. Davin, M. Hirschi, E. B. Jaeger, I. Lehner, B. Orlowsky, and A. J. Teuling (2009), Investigating soil moisture-climate interactions in a changing climate: A review, *Earth-Science Reviews* (revised).

[17] Teuling, A. J., M. Hirschi, A. Ohmura, M. Wild, M. Reichstein, P. Ciais, N. Buchmann, C. Ammann, L. Montagnani, A. D. Richardson, G. Wohlfahrt, and S. I. Seneviratne (2009), A regional perspective on trends in continental evaporation, *Geophys. Res. Lett., 36*, L02404, doi:10.1029/2008GL036584.

[18] Uppala, S. M., et al. (2005), The ERA-40 reanalysis, *Q. J. R. Meteorol. Soc., 131*, 2961-3012.

[19] Vautard, R., P. Yiou, F. D'Andrea, N. de Noblet, N. Viovy, C. Cassou, J. Polcher, P. Ciais, M. Kageyama, and Y. Fan (2007), Summertime European heat and drought waves induced by wintertime Mediterranean rainfall deficit, *Geophys. Res. Lett., 34*, L07711, doi:10.1029/2006GL028001.

[20] Wild, M., H. Gilgen, A. Roesch, A. Ohmura, C. Long, E. Dutton, B. Forgan, A. Kallis, V. Russak, and A. Tsvetkov (2004), From dimming to brightening: Decadal changes in solar radiation at the Earth's surface, *Science, 308*, 847-850.